Title
Strain to alter the covalency and superconductivity in transition metal diborides

Journal
Journal of Materials Chemistry C, 7(34)

ISSN
2050-7526

Authors
Zhai, Huanchen
Munoz, Francisco
Alexandrova, Anastassia N

Publication Date
2019-08-29

DOI
10.1039/c9tc02095k

Peer reviewed

ARTICLE

Strain to Alter the Covalency and Superconductivity in Transition Metal Diborides

Received 00th January 20xx,
Accepted 00th January 20xx

DOI: 10.1039/x0xx00000x

Huanchen Zhai,[1] Francisco Munoz,[2,3,*] Anastassia N. Alexandrova[1,4,*]

Among layered metal diborides, MB_2, only MgB_2 is a superconductor. We explicate the details of the chemical bonding in the diboride series, and, based on those, propose a strategy for the application of anisotropic mechanical stress that could lead to the superconducting behavior in some transition metal diborides, particularly in ScB_2. The key aspect detrimental to superconductivity is found to be the covalent metal-boron bonding enabled by the presence of d-electrons on the metal. We show that, based on the differential response to electronic states of different angular momenta to anisotropic strain or compression, the covalent overlap can be strategically manipulated. The metal-boron covalency in ScB_2 can be removed when the lattice is compressed along the *ab*-direction, or stretched along the *c*-direction. Both types of stress are characterized by the rise of the degenerate σ-band toward crossing the Fermi level. The elongation along *c* also softens the degenerate E_{2g} phonon that can split this s-band to produce Cooper pairs. More generally, while the effect of mechanical stress on superconductivity has been seen before, it was not known what exactly the stress achieves. Here we explicate this on the example of a particular alloy family. Our findings can lead to strategies for choosing the type and strength of mechanical stress for the manipulation of materials' vibronic structures toward superconductivity.

Introduction

It would be great if novel superconductors could be discovered other than by serendipity. In this contribution we report one lever in the material electronic and vibrational structure that could be instrumental in manipulating superconductive behavior. We focus on a family of metal diborides, MB_2. MgB_2 stands out in this series, as well as in general among superconducting materials at the ambient pressure, for its critical temperature (T_c) is the highest among conventional superconductors.[1] However, there are several transition metal diborides with the same crystalline structure, albeit not superconductors, or having much lower T_c.[2] Several studies offer theoretical explanations of the low T_c or lack of superconductivity in these materials, but no uniform theory of the trends present in MB_2 emerges so far.[3] Additionally, most of these works offer little or no insight into the chemical bonding and molecular level detail that would clearly differentiate the known MB_2 phases.

In this article, we explicate the differences in the electronic and phonon structures in MgB_2 and several transition metal diborides, which lead to the presence or absence of superconducting behavior in these seemingly similar materials. Having understood the principal difference that leads to the absence of superconductivity in transition metal diborides, we propose a way to manipulate the chemical bonding and vibrations in them through strain. In the case of ScB_2, we succeed to manipulate the electronic structure and vibrations through strain so that it starts to mimic those in MgB_2. While strain has been occasionally reported as a factor that can lead to the onset of superconducting behavior,[4-10] this effect was found serendipitously and no rationale was provided. Here, we show what can be achieved through strain on the level of chemical bonds. We show that strain can be chosen strategically to alter the degree of atomic orbital (AO) hybridization, and thus reduce the covalency of specific bonds in the crystal lattice. This effect can be used to shift the energies of electronic and vibrational states and increase the e-ph coupling, leading to the onset of superconductivity.

Results and discussion

Metal diborides in the absence of strain. We begin from MgB_2, a superconductor with high T_c (Fig. 1).[1] Currently, several efforts are carried to control its properties and synthesis.[11-17] The mechanism behind its superconductivity is well-understood as driven by the electron-phonon interaction.[18,19] The band structure of MgB_2 at equilibrium (Fig. 1a) shows two bands crossing the Fermi level, making MgB_2 a two-gap

[1]*Department of Chemistry and Biochemistry, University of California, Los Angeles, Los Angeles, CA, 90095, USA*
[2]*Departamento de Física, Facultad de Ciencias, Universidad de Chile, Chile*
[3]*Center for the Development of Nanoscience and Nanotechnology CEDENNA, Santiago, Chile*
[4]*California NanoSystems Institute, Los Angeles, CA, 90095, USA*
**Corresponding authors emails:*
Francisco Munoz: fvmunoz@gmail.com,
Anastassia N. Alexandrova: ana@chem.ucla.edu
Electronic Supplementary Information (ESI) available: [details of any supplementary information available should be included here]. See DOI: 10.1039/x0xx00000x

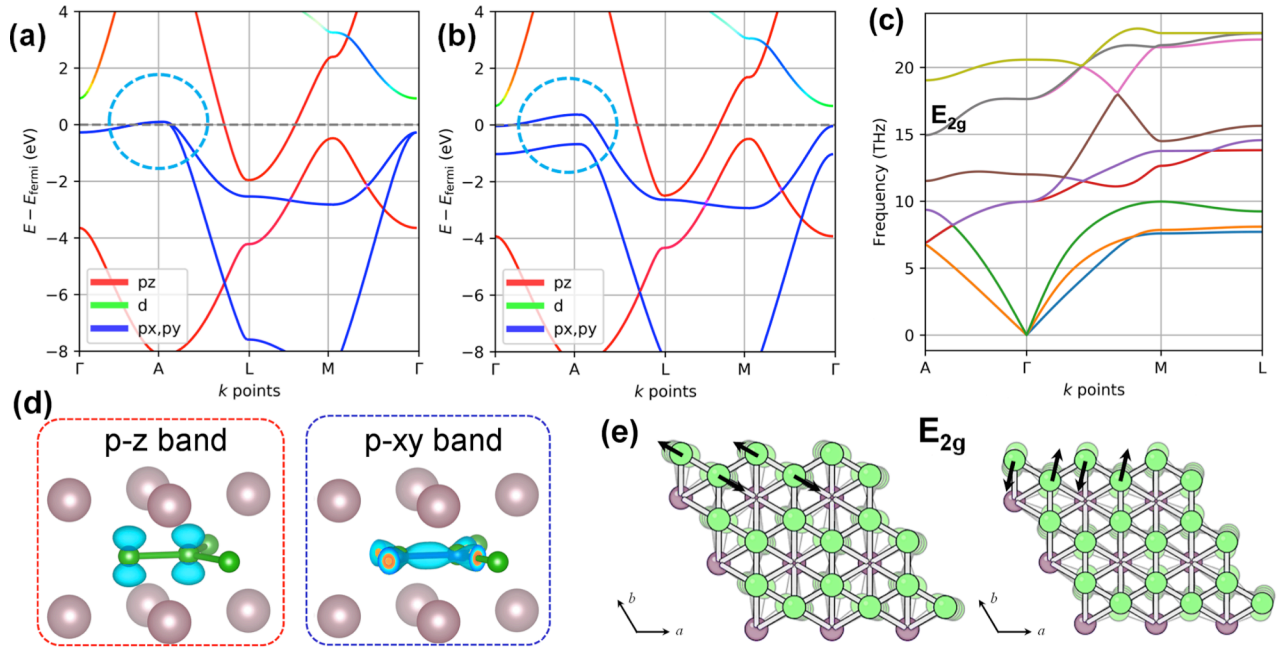

Figure 1. MgB_2 (a) band structures with the σ-band (p-xy) shown in blue and the π-band (p-z) shown in red; the Cartesian system in use has the z-direction aligned with the *c* direction of the unit cell, and xy are in the *ab* plane. (b) changes in the band structures after the frozen E_{2g} phonon of the amplitude of 0.04 Å is applied; the light blue circle highlights the splitting of the σ-band important for superconductivity; (c) phonon dispersion, with the E_{2g} phonon that distorts the σ B-B bonds labeled; (d) charge density for the π- and σ-bands at the Γ point; (e) the normal node displacements of atoms in the lattice corresponding to the degenerate E_{2g} phonon.

superconductor.[20-22] The bands of the π symmetry (Fig. 1a,d) cross the Fermi level at the borders of the hexagonal Brillouin zone. The phonon structure is shown in Fig. 1c. No phonon mode is effective in distorting the Fermi surface of the π symmetry. However, the σ-band (Fig. 1a,d), whose Fermi surface pierces the Brillouin zone from Γ to A, and is degenerate along that line and very close to the Fermi level. Appropriate phonons can break the symmetry associated with this band degeneracy, and produce the energy splitting. The phonon that can accomplish this is the σ B–B bonds stretching phonon of the E_{2g} symmetry (Fig. 1c,e). By applying a frozen E_{2g} phonon (i.e. a displacing the atoms in the lattice along the normal mode vector), a large distortion of the σ-band is achieved near the Fermi level (Fig. 1b, blue outline). Transient pairing of electrons in the lower of the formerly-degenerate σ-states, and state reordering through the E_{2g} vibration is the mechanism behind the creation of the Cooper pairs. In addition to the changes on the electronic structure (or the deformation potential), the E_{2g} phonon is quite anharmonic, and this increases T_c even further.[18] In summary, the σ-band and its electron-phonon interaction with the E_{2g} phonon are responsible of the unusually high T_c found in MgB_2. The π band, which also has a superconducting gap, decreases T_c by a residual scattering among Cooper pairs.[23]

Upon replacing Mg in MgB_2 with early transition metals, Sc, Y, Ti, Zr, V, Mo, Cr, and Nd, several changes happen in the electronic structure (Figures 2, and S1 in the Supporting Information). The σ- and π-bands can be recognized. However, as the number of electrons in the system increases, the Fermi level goes up. In ScB_2 and YB_2 the σ-band is not fully occupied, but at Γ it is below the Fermi level, changing the topology of the Fermi surface with respect to that in MgB_2. For metals to the right of Ti and Zr, the σ-band is completely occupied. Hence, the solids lose the ability to split the degeneracy of this band through e-ph coupling. Additionally, in MB_2, the dispersion of the σ-bands is increased along the Γ–A line, as compared to MgB_2. The dispersion in this direction indicates an increase in hybridization and covalent bonding between the boron and the orbitals on the metal. The π-band hybridizes with the metal d-bands at higher energies. The nature and strength of hybridization depends on the metal in a complicated way.

Covalent bonding also affects the phonons (Figure 2). In particular, the E_{2g} phonon loses dispersion along A–Γ in all MB_2 alloys, in contrast to that in MgB_2. The phonon energy increases from $\omega(A)$=15.1, $\omega(\Gamma)$=18.7 THz in MgB_2 (Figure 1c), to ω~27 THz in TiB_2, for example, indicating the strengthening of the material. Shifting both the σ-bands the E_{2g} phonon through metal-boron bonding reduces their electron-phonon (e-ph) coupling. Indeed, the frozen E_{2g} phonon, which causes the splitting of σ-bands in MgB_2 at Γ on the order of 1.1 eV at the 0.02 Å amplitude, induces a splitting of 0.7 eV in ScB_2 and TiB_2. Hence, we see that the key factors detrimental to superconductivity in transition metal diborides is the covalent character of the metal-boron bonding, as well as the number of d-electrons populating the σ-band. The lattice parameter *c*

nearly perfectly linearly correlates with the number of d-electrons as well as the electronegativity of the metal, in the series, Sc, T, V, Cr, and Y, Zr, Nb, Mo (Figure S2). Indeed, the electronegativity of Mg (1.31) is very far from that of B (2.04), whereas Mo (2.16) is very close to B, clearly making MoB_2 more covalent than MgB_2. All other MB_2 alloys fall in-between MoB_2 and MgB_2, in terms of the covalency of bonding, Sc and Y being the closest. Hence, covalency of bonding is responsible for shortening of the lattice in the z-direction, as expected for stronger covalent interactions. The number of d-electrons additionally systematically shifts the E_F to the right in the Periodic Table.

Removing covalency through mechanical stress. Hence, reducing the degree of covalency of the metal-boron bonding, and shifting electrons from the overly-populated σ-band to other bands could potentially recreate the superconducting behavior in diborides. We hypothesize now that this effect could be achieved through specifically applied mechanical stress. We showed in the past that orbitals of different angular momenta respond to mechanical stress differently.[24] For example, in diatomic molecules, compression along the bond axis typically destabilizes the σ-bond due to increasing electron-electron repulsion. On the other hand, the π- and especially the δ- and the ϕ-bonds may drop in energy upon moderate compression, because the otherwise poor bonding

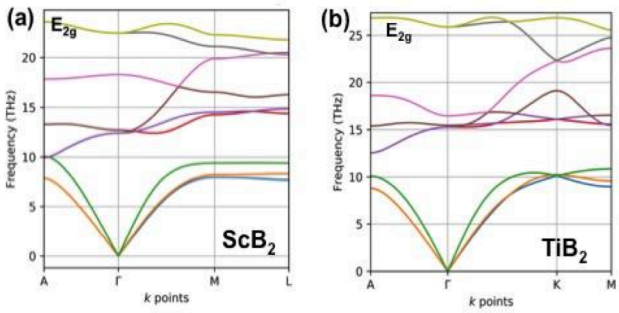

Figure 2. Phonon spectra of ScB_2 and TiB_2 at equilibrium. The E_{2g} phonon is labeled.

overlap would be enhanced at a shorter internuclear separation (Figure S3). Antibonding states would all go up in energy upon compression, but states of the lower angular momentum would go up more quickly. Strain along a bond would generally destabilize the bonding states and stabilize the antibonding states, but the rate with which the states shift in energy as a function of strain is again angular-momentum dependent.

Drawing from this argument, we propose the first strategy to manipulate the vibronic structure of MB_2. The critical state to manipulate is the boron σ-band, which, through the higher population and covalency with the metal, dropped too low in energy. Given that electronic states of lower angular momenta quickly rise in energy upon compression, we hypothesize that

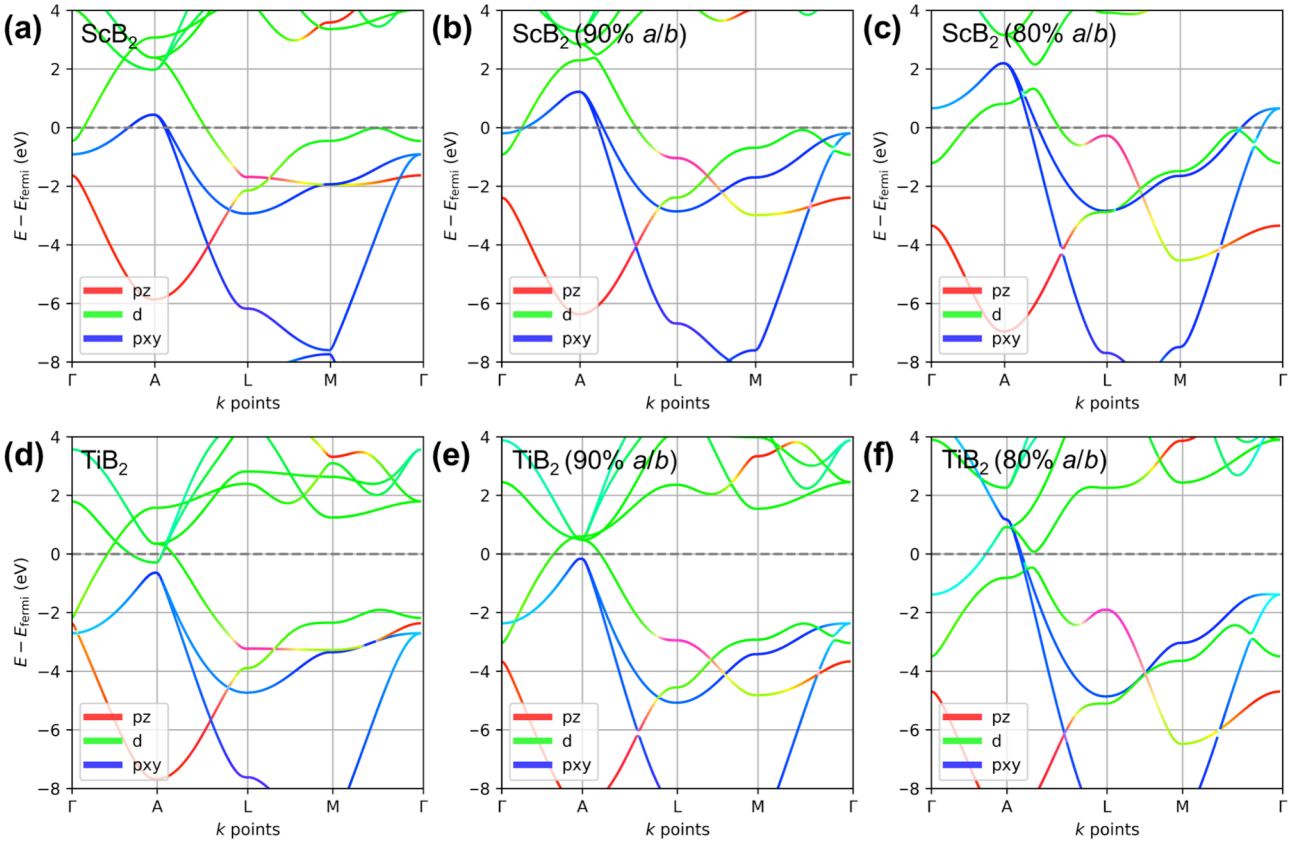

Figure 3. The band structures of (a-c) ScB_2 and (d-f) TiB_2 with cell parameters along *a* and *b* direction being 100%, 90%, and 80% (from left to right). The optimized cell parameters *a* and *b* are 3.1457 and 3.0351 Å, respectively.

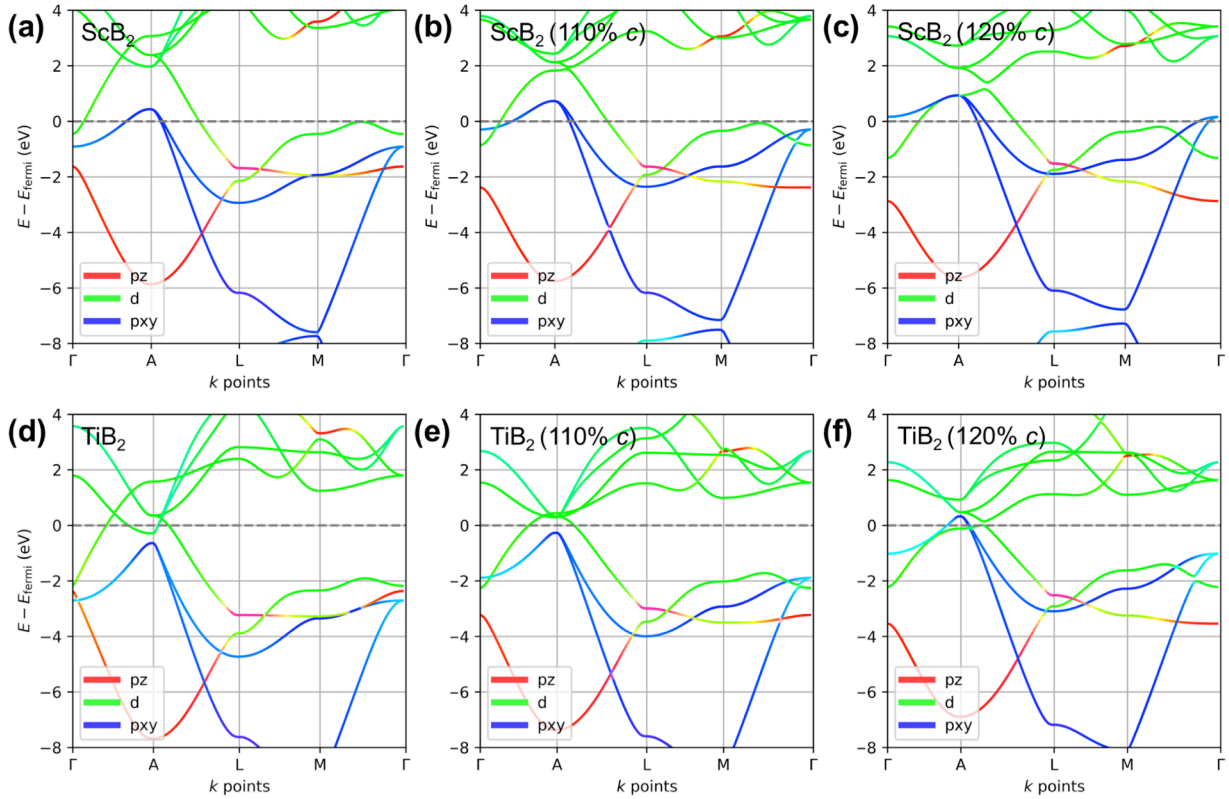

Figure 4. The band structures of (a-c) ScB_2 and (d-f) TiB_2 with cell parameters along *c* direction being 100%, 110%, and 120% (from left to right). The optimized cell parameters *c* are 3.5242 and 3.2232 Å, for ScB_2 and TiB_2, respectively.

compressing MB_2 in the *ab* plane should push the σ-band up, while the π-band might get stabilized due to enhanced π-overlap. This may be additionally facilitated by the uncoupling of the σ-band from any hybridization with the sd-states on the metal. The aim is to make the σ-band rise above the Fermi level, while extra electrons would populate the π-states that would simultaneously undergo stabilization. We focus on the most promising earlier transition metal diborides ScB_2 and TiB_2, whose electronic structure is closest to that of MgB_2. YB_2 and ZrB_2 are also interesting, but their electronic structure is more complicated due to the onset of relativistic effects, and so we omit them in this study. The band structures of ScB_2 and TiB_2 under compression along *ab* are shown in Figure 3. We indeed succeed in pushing the σ-bands up toward the Fermi level, but only in ScB_2: at 10% compression, most of the band rises above the Fermi level along the *A*-*Γ* line, and at 20% it becomes fully unoccupied. Apart from having a more pronounced dispersion, the σ-band in 20% compressed ScB_2 resembles that of MgB2 quite closely (Figure 1). The TiB2 case remains below E_F and also shows a more persistent hybridization with the orbitals on the Ti. As the σ-band rises in energy, its population shifts, but the charges on atoms calculated using the Bader formalism[25] remain essentially unchanged, indicating that the population shifted primarily to the π-band, in accord with our hypothesis.

An alternative way of shifting the boron σ-band up is to act on the metal-boron bonds, and decouple the states of the metal and the boron from the covalent overlap in this way. There are two aspects affecting the quality of the covalent overlap: The first one is the geometric separation of the covalent partners; as with the compression along *ab*, modification of the *c* parameter of the lattice (i.e. pushing together or pulling apart the metal and the boron layers) should shift the covalent states in energy. Secondly, the covalent bonding is facilitated by the sd-hybridization of atomic orbitals (AOs) of the transition metal, since AO-hybridization anisotropically increases the size the orbital and enhances the covalent overlap.[26] Stretching MB_2 along c should lead to energy separation between s- and d-AOs on the metal, as they would lose the covalent overlap with the boron with different rates.[24] The difference would be subtle, because in Sc and Ti the 4s and 3d-AOs are quite close in energy. The band structures of ScB_2 and TiB_2 before and after elongation along the z direction are shown in Figure 4. We see that the elongation can indeed shift the σ-band up. However, again, only for the ScB_2 case can the σ-band be pushed to the Fermi level. At 20% elongation the band looks similar to that of MgB_2 along *A*-*Γ*. The fact that the σ-band in TiB_2 remains below E_F upon stretching of the lattice can be explained by the fact that the c parameter of TiB_2 is much shorter than that of ScB_2 or MgB_2, in line with a greater covalent character of bonding between Ti and B, and the significantly higher E_F in TiB_2. Elongation shifts some electrons from the rising σ-band to the metal (Table S1).

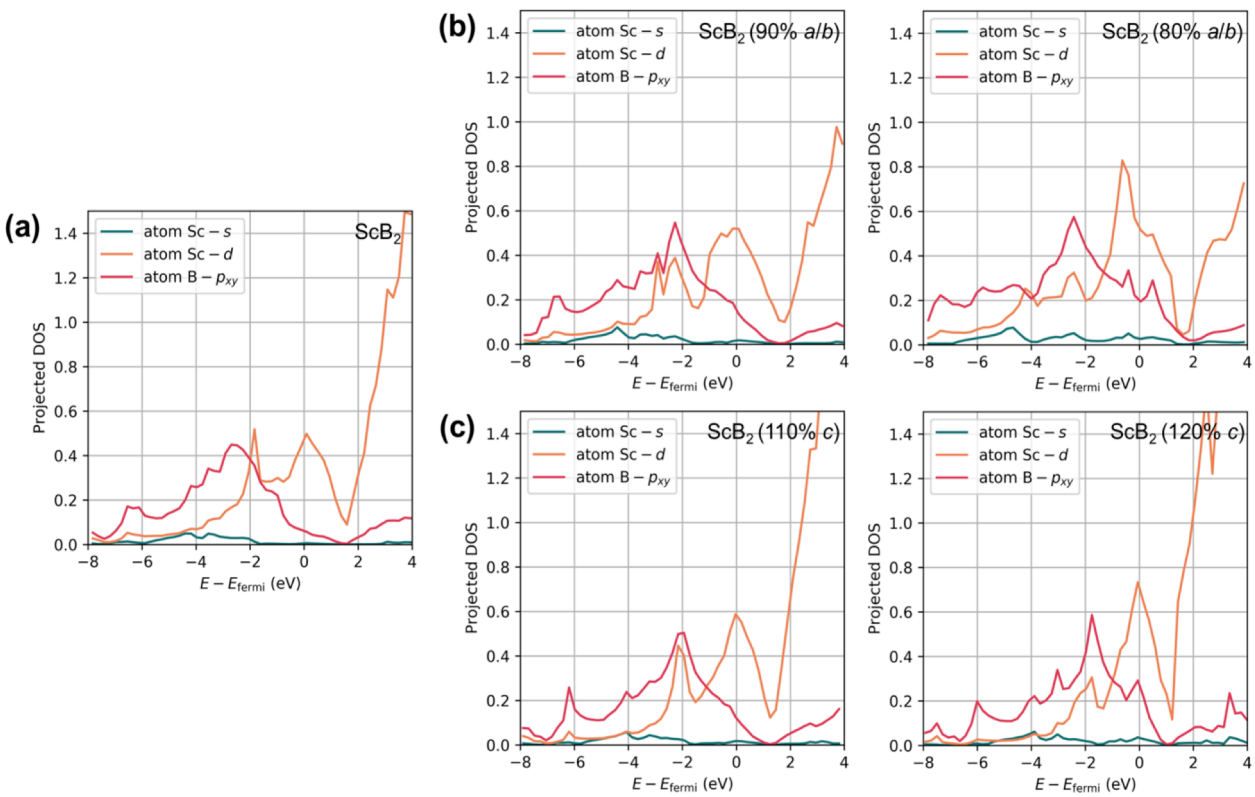

Figure 5. Projected DOS of ScB_2 (a) equilibrium structure, (b) the structure with compressed along *ab*, and (c) the structure elongated along *c*. The boron σ-states formed by the boron p_{xy}-AOs (red) shift toward the Fermi level upon both types of cell deformations. The s- and d-states of Sc (teal and orange, respectively) rise in energy and develop peaks at the Fermi level upon lattice deformations.

We focus now on the more promising case of ScB_2. The density of states (DOS) projected on the orbitals of B and Sc, for the optimized and stressed along *c* and *ab* ScB_2 are shown in Figure 5. It can be seen that the boron σ-states shift toward the Fermi level after the cell parameter elongation along the *c* direction. Additionally, the s- and d-states on Sc show pronounced differences before and after elongation. Upon elongation, the Sc s-states rise in energy and gradually develop a peak near the Fermi level (teal in Figure 5). The effect of the compression along *ab* on the p-DOS is nearly identical, again showing the important build-up of the boron σ-states at E_F.

The effect of cell parameter change on the band shifting of metal borides has also been found in other studies, both experimentally and computationally, but without a chemical bonding rationale.[27,4,28] Band structure of MgB_2 will change and the superconducting transition temperature T_c will be raised if the c parameter is increased.[27] An experimental study states that the high c lattice constant (c = 3.52 Å) of MgB_2 should explain its high T_c, comparing to $NbB_{2.4}$ (c = 3.32 Å) and AlB2 (c = 3.25 Å).[4] Another experimental study shows that for NbB_{2+x} system, increasing x gradually from 0 to 1 increases the cell parameter *c*, and at the same time T_c also increases with a similar trend.[28] Our findings agree with, and expand upon these earlier observations, and substantiate them with the electronic and vibrational information. Additionally, we so far see that the compression along *ab* achieves the same effect on the electronic structure as the elongation along *c*.

To summarize, both proposed types of mechanical stress are effective in raising the boron σ-band and decreasing its population, when applied to ScB_2. Depending on the associated behavior of the E_{2g} phonon, the e-ph coupling might be enabled again.

Stress and phonon structure. As the boron states loosen the grip of covalency with the metal, would the E_{2g} phonon recover its smaller frequency? We test this for both the promising ScB_2 case, and the not-promising TiB_2, as these two materials have the electronic and vibrational structures of the highest initial resemblance to those of MgB_2.

After significantly changing the lattice constants via mechanical stress, TiB_2 is found to lose the original symmetry, i.e. gain imaginary phonons (Supporting Information). However, for ScB_2, the structure is found to remain after applying both types of studied deformations. Figure 6 shows the phonon spectra of ScB_2 before and after compressing along *ab* and increasing the *c* parameter. After increasing *c* parameter, the E_{2g} phonon band became much lower in energy along the *Γ-A* line. This correlation between *c* lattice constant and phonons should enable the e-ph coupling, and create an experimentally observable change in T_c. However, the compression along *ab* made the phonon rise in energy along

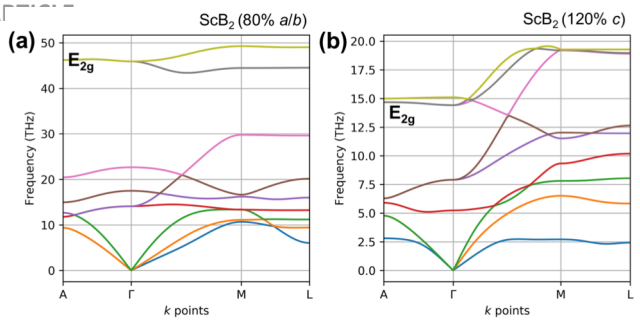

Figure 6. Phonon spectra of ScB_2 upon applied compression along *ab*, and elongation along *c*. The yellow band in (a) and (b) or gray band in (c) from A to Gamma *k*-points is the E_{2g} band. Upon the *ab* compression, the band rises in energy. Upon the elongation along *c*, it drops in energy at *Γ*.

the *Γ-A* line. This effect is likely due to the increased π-overlap upon compression, making the lattice stiffer in the xy plane. Hence, while the compression has the desired effect on the σ-band, it does not help the e-ph coupling with the E_{2g} phonon. Only the elongation along *c* remains a promising mode of mechanical deformation. Both the electronic and the vibrational structures of ScB_2 start looking like those of MgB_2 upon the elongation. This suggests that superconducting behavior could be observed in anisotropically stressed ScB_2.

Effect of doping. One of the most explored ways to control or even induce superconductivity is the doping. This is also the case of MgB_2 and MB_2 materials. There is a large wealth of evidence relating the doping of MgB_2 to changes of the lattice parameters and to the change of the Tc. In it is generally found that a small amount of substitutional doping of a transition metal decreases both, the c lattice parameter and the Tc.[29-31] There are few exceptions, in the case of slightly Co doped MgB2, both the lattice parameters and Tc remains almost constant,[32] and in the case of Sc doping, the main changes are an increase of the lattice parameter together with the decrease of the Tc.[33] All the aforementioned trends are in line with the effect of the different types of strain in our article.

Regarding MB2 materials, there are few reports of superconductivity induced due doping. Renosto et al.[34] and Barbero et al.[35] found the emergence of superconductivity in V-doped ZrB2 and HfB2. They measured a decrease of the c lattice parameter due to the doping. This suggests that in this case the change of the c-parameter is not the key factor for the onset of superconductivity. Instead, the superconductivity in these systems can be explained by two factors (i) the V doping moves downwards in energy (respect to the Fermi energy) the d bands (ii) the V impurity splits the dxz, dyz bands, the lower branch of these bands is degenerated, semi-filled and almost flat along the *Γ-A* line. Therefore, upon the V-doping the dxz-dyz bands behave in a similar way to the σ-band of MgB_2. The related calculations are presented in the Supplementary Material.

Finally, it is worth to mention that the excess of B also can induce superconductivity. As in the case of doped MgB_2, this is related to increasing the c-axis.[36,37]

Computational Methods

The ScB_2 and TiB_2 atomic configurations are obtained from *Materials Project*.[38] DFT calculations are performed using VASP 5.4.4,[39,40] with PBE functional,[41] energy cutoff equal to 500 eV, and *k*-points grid 15x15x15 centered at Gamma point. The optimized lattice constants are $a = b = 3.1457$ Angstrom and $c = 3.5242$ Angstrom for ScB_2, and $a = b = 3.0351$Angstrom and $c = 3.2232$ Angstrom for TiB_2, respectively. For structure optimization, the lattice constants are relaxed and tetrahedron smearing method with Blöchl corrections is used. For band structure plotting Gaussian smearing is used. The phonon calculations are performed using Phonopy 1.13.2[42] and VASP 5.4.4. For phonon calculation, a 4x4x3 (for MgB_2) and 4x4x4 (for TiB_2 and ScB_2) super cell is used. Based on the geometry super cell, two structures with displacements are generated for calculating forces. The forces of these super cell structures are evaluated using 11x11x11 k point mesh. The unfolding of the band structures is made with the pyProcar code.

Conclusions

In summary, in this contribution we explicate how superconductivity in a series of related materials, metal diborides, can be understood and strategically manipulated on the level of chemical bonds. In these layered materials, the σ-bonding states on the boron need to be located at the Fermi level, be partially occupied, and couple to the low-frequency anharmonic E_{2g} phonon, for the creation of the superconducting Cooper pairs. This is achieved in MgB_2, where the Mg-B bonding is purely ionic. In all transition metal diborides, the occupied d-AOs of the metal participate in the bonding and bring covalent character to the metal-boron bonds. This, together with the larger number of electrons in the systems, pulls down the σ-band and the same time stiffens the E_{2g} phonon, diminishing their e-ph coupling. We tested two mechanisms by which the metal-boron covalency could be manipulated. We showed that stretching the material uniaxially along the c-axis decouples the sd-hybrid on the metal and the hybrid from the bonds with the boron. This raises the energy of the σ-band, making it half-full at certain degree of strain. The loss of covalent character also reduces the frequency of the E_{2g} phonon. Upon the compression along the *ab*-direction in the lattice, the σ-band also quickly rises in energy due to electron-electron repulsion in this low-angular momentum state, and additional deterioration of the metal-boron bonding overlap. The compressed lattice favors the π-overlap, and so electron population shifts to the π-band. However, the latter acts against the desired softening of the E_{2g} phonon, and hardens it instead as the lattice becomes stiffer in the xy-plane.

We thus propose one type of mechanical stress, chosen through the analysis of chemical bonding, such that the e-ph coupling should become enabled again in ScB_2, and mimic that in MgB_2. We note that not every diboride is able to withstand

the types of mechanical stress proposed, without changing structure.

The effect of mechanical stress on superconductivity has been explored. Usually, extreme pressures are considered, and new superconducting phases are predicted to form in those conditions. For materials having the structure corresponding to ambient conditions, the effect of mechanical stress was also observed, and came as a surprise. Our work points at the specific chemical bonding and vibronic effects that strain can cause. Thus, we may begin envisioning more general recipes for choosing the direction and strength of mechanical stress for strategically manipulating the electronic and vibrational properties of a material toward the onset of superconductivity. Specifically, one would want to identify the degenerate electronic states that could be split by an appropriate phonon, but lie too low in energy. These states could be brought to the Fermi level by a strain that decouples the covalency within these states. Additionally, the removal of covalency would affect the frequency of the phonon of interest. Thus, strain would have to be chosen to strike the balance between electron and phone energies.

Conflicts of interest

There are no conflicts to declare.

Acknowledgements

Financial support comes from the NSF-CAREER Award CHE-1351968 to A.N.A.. F.M. was funded by FONDECYT Grants 1150806 and 1191353, and the Center for the Development of Nanoscience and Nanotechnology CEDENNA FB0807. We also acknowledge the XSEDE for computational resources.

References

1. Nagamatsu, J.; Nakagawa, N.; Muranaka, T.; Zenitani, Y.; Akimitsu, J. Superconductivity at 39 K in magnesium diboride. *Nature* **2001**, *410*, 63-64.

2. Heid, R.; Bohnen, K.-P.; Renker, B. Electron-phonon coupling and superconductivity in MgB_2 and related diborides. In Adv. Solid State Phys., pp. 293-305. Springer, Berlin, Heidelberg, 2002.

3. Medvedeva, N. I.; Ivanovskii, A. L.; Medvedeva, J. E.; Freeman, A. J. Electronic structure of superconducting MgB_2 and related binary and ternary borides. *Phys. Rev B.* **2001**, *64*, 020502.

4. Mudgel, M.; Awana, V. P. S.; Kishan, H.; Felner, I.; Alvarez, G. A.; Bhalla, G. L. Superconductivity of various borides: The role of stretched c-parameter. *J. Appl. Phys.* **2009**, *105*, 07E313.

5. Bekaert, J.; Aperis, A.; Partoens, B.; Oppeneer, P. M.; Milošević, M. V. Evolution of multigap superconductivity in the atomically thin limit: Strain-enhanced three-gap superconductivity in monolayer MgB_2. *Phys. Rev. B.* **2017**, *96*, 094510.

6. Pogrebnyakov, A. V.; Redwing, J. M.; Raghavan, S.; Vaithyanathan, V.; Schlom, D. G.; Xu, S. Y.; Li, Q.; Tenne, D. A.; Soukiassian, A.; Xi, X. X.; Johannes, M. D. Enhancement of the Superconducting Transition Temperature of MgB_2 by a Strain-Induced Bond-Stretching Mode Softening. *Phys. Rev. Let.* **2004**, *93*, 147006.

7. Zheng, J. C.; Zhu, Y. Searching for a higher superconducting transition temperature in strained MgB_2. *Phys. Rev. B.* **2006**, *73*, 024509.

8. Xiao, R.C.; Lu, W.J.; Shao, D.F.; Li, J.Y.; Wei, M.J.; Lv, H.Y.; Tong, P.; Zhu, X.B.; Sun, Y.P. Manipulating superconductivity of 1T-TiTe2 by high pressure. J. Materials Chem. C 2017, 5, 4167-4173.

9. Yao, Y.; Tse, J.S. Superconducting hydrogen sulfide. Chem.: Eur. J. 2018, 24, 1769-1778.

10. Drozdov, A.P.; Eremets, M.I.; Troyan, I.A.; Ksenofontov, V.; Shylin, S.I. Conventional superconductivity at 203 kelvin at high pressures in the sulfur hydride system. Nature 2015, 525, 73.

11. Liu, Y.; Cheng, F.; Qiu, W.; Ma, Z.; Al Hossain, M.S.; Dou, S.X. High performance MgB2 superconducting wires fabricated by improved internal Mg diffusion process at a low temperature. J. Mater. Chem. C 2016, 4, 9469-9475.

12. Cheng, F.; Liu, Y.; Ma, Z.; Al Hossain, M.S.; Somer, M. The isotope effect of boron on the carbon doping and critical current density of Mg11B2 superconductors. J. Mater. Chem. C 2017, 5, 663-668.

13. Liu, S.; He, R.; Xue, L.; Li, J.; Liu, B.; Edgar, J.H. Single Crystal Growth of Millimeter-Sized Monoisotopic Hexagonal Boron Nitride. Chem. Mater. 2018 30, 6222-6225.

14. Cheng, F.; Ma, Z., Yu; L., Li; C., Liu; C.; Guo, Q.; Li, H.; Yamauchi, Y.; Bando, Y.; Alghamdi, Y.G.; Alshehri, A.A. Effects of morphology of Mg powder precursor on phase formation and superconducting properties of Mg11B2 low activation superconductor. J. Mater. Chem. C 2018, 6, 8069-8075.

15. Li, W.; Kang, J.; Liu, Y.; Zhu, M.; Li, Y.; Qu, J.; Zheng, R.; Xu, J.; Liu, B. Extrinsic Two-dimensional Flux Pinning Centers in MgB2 Superconductor Induced by Graphene-Coated Boron. ACS Appl. Mater. Interfaces 2019, 11, 10818-10828.

16. Yeoh, W.K.; Cui, X.Y.; Gault, B.; De Silva, K.S.B.; Xu, X.; Liu, H.W.; Yen, H.W.; Wong, D.; Bao, P.; Larson, D.J.; Martin, I. On the roles of graphene oxide doping for enhanced supercurrent in MgB2 based superconductors. Nanoscale 2014, 6, 6166-6172.

17. Fang, F.; Iyyamperumal, E.; Chi, M.; Keskar, G.; Majewska, M.; Ren, F.; Liu, C.; Haller, G.L.; Pfefferle, L.D. Templated one-step catalytic fabrication of uniform diameter MgxBy nanostructures. J. Mater. Chem. C 2013, 1, 2568-2576.

18. Yildirim, T.; Gülseren, O.; Lynn, J. W.; Brown, C. M.; Udovic, T. J.; Huang, Q.; Rogado, N.; Regan, K. A.; Hayward, M. A.; Slusky, J. S.; He, T. Giant anharmonicity and nonlinear electron-phonon coupling in MgB_2: a combined first-principles calculation and neutron scattering study. *Phys. Rev. Lett.* **2001**, *87*, 037001.

19. Choi, H. J.; Roundy, D.; Sun, H.; Cohen, M. L.; Louie, S. G. The origin of the anomalous superconducting properties of MgB_2. *Nature* **2002**, *418*, 758-760.

20. Xi, X. X. Two-band superconductor magnesium diboride. *Rep. Prog. Phys.* **2008**, *71*, 116501.

21. Chen, X, K,; Konstantinović, M. J.; Irwin, J. C.; Lawrie, D. D.; Franck, J. P. Evidence for two superconducting gaps in MgB_2. *Phys. Rev. Lett*. **2001**, *87*, 157002.

22. Chen, K.; Dai, W.; Zhuang, C. G.; Li, Q.; Carabello, S.; Lambert, J. G.; Mlack, J. T.; Ramos, R. C.; Xi, X. X. Momentum-dependent multiple gaps in magnesium diboride probed by electron tunnelling spectroscopy. *Nat. Commun.* **2012**, *10*, 669.

23. Pickett, W. Superconductivity: Mind the double gap. *Nature* **2002**, *418*, 733.

24. Robinson, P. J.; Alexandrova, A. N. Assessing the bonding properties of individual molecular orbitals. *J. Phys. Chem. A* **2015**, *119*, 12862-12867.

25. Henkelman, G.; Arnaldsson, A.; Jónsson, H. A fast and robust algorithm for Bader decomposition of charge density. *Comput. Mater. Sci.* **2006**, *36*, 354-360.

26. Pauling, L. *The Nature of the Chemical Bond.* Vol. 260. Ithaca, NY: Cornell university press, 1960.

27. Wan, X.; Dong, J.; Weng, H.; Xing, D. Y. Band structure of MgB_2 with different lattice constants. *Phys. Rev. B* **2001**, *65*, 012502.
28. Awana, V. P. S.; Vajpayee, A.; Mudgel, M.; Kishan, H. Superconductivity of various borides and the role of carbon in their high performance. *Supercond. Sci. Technol.* **2009**, *22*, 034015.
29 Mudgel, M.; Awana, V. P. S.; Bhalla, G. L.; Kishan, H. Superconductivity of Nb1−x Mg x B2: Impact of Stretched c-Parameter. *J. Supercond. Nov. Magn*. **2008**, *21*, 457-460.
30 Zhang, H.; Zhao, J.; Shi, L. The charge transfer induced by Cr doping in MgB2. *Physica C Supercond.* **2005**, *424*, 79-84.
31. Mudgel, M.; Awana, V. P. S.; Kishan, H.; Felner, I.; Alvarez, G. A.; Bhalla, G.L. Superconductivity of various borides: The role of stretched c-parameter. *J. Appl. Phys*. **2009**, *105*, 07E313.
32. Shi, L.; Zhang, S.; Zhang, H. Effects of Co and Mn doping on the structure and superconductivity of MgB2. *Solid state Commun*. **2008**, *147*, 27-30.
33. Agrestini, S.; Metallo, C.; Filippi, M.; Campi, G.; Sanipoli, C.; De Negri, S.; Giovannini, M.; Saccone, A.; Latini, A.; Bianconi, A. Sc doping of MgB2: the structural and electronic properties of Mg1−xScxB2. *J. Phys. Chem. Solids* **2004**, *65*, 1479-1484.
34. Renosto, S. T.; Consoline, H.; dos Santos, C. A. M.; Albino Aguiar, J.; Jung, Soon-Gil; Vanacken, J.; Moshchalkov, V. V.; Fisk, Z.; Machado, A. J. S. Evidence of multiband behavior in the superconducting alloy Zr0.96V0.04B2. *Phys Rev. B* **2013**, *87*, 174502.
35. Barbero, N.; Shiroka, T.;Delley, B. Grant, T. Machado, A. J. S.; Fisk Z.; Ott H.-R.; and Mesot, J. Doping-induced superconductivity of ZrB2 and HfB2. *Phys. Rev. B* **2017**, *95*, 094505.
#6. Escamilla, R.; Lovera, O.; Akachi, T.; Durán, A.; Falconi, R.; Morales F.; Escudero, R. Crystalline structure and the superconducting properties of NbB2+x. *J. Phys.: Condens. Matter* **2004**, *16*, 5979.
37. Takagiwa, H.; Nishibori, E.; Okada, N.; Takata, M.; Sakata M.; Akimitsu, J. Relationship between superconductivity and crystal structure in NbB2+x, *Sci. Technol. Adv. Mater*. **2006**, *7*, 22-25.
38. Jain, A.; Ong, S. P.; Hautier, G.; Chen, W.; Richards, W. D.; Dacek, S.; Cholia, S.; Gunter, D.; Skinner, D.; Ceder, G.; Persson. K. A. Materials Project: A materials genome approach to accelerating materials innovation. *APL Materials* **2013**, *1*, 011002.
39 Kresse, G.; Furthmüller, J. Efficient iterative schemes for ab initio total-energy calculations using a plane-wave basis set. *Phys. Rev. B* **1996**, *54*, 11169−11186.
40. Blöchl, P. E. Projector augmented-wave method. *Phys. Rev. B* **1994**, *50*, 17953−17979.
41. Perdew, J. P.; Burke, K.; Ernzerhof, M. Generalized Gradient Approximation Made Simple. *Phys. Rev. Lett.* **1996**, *77*, 3865−3868.
42. Togo, A.; Tanaka, I. First principles phonon calculations in materials science. *Scr. Mater.* **2015**, *108*, 1-5.

